A&A 497, 243–253 (2009)
DOI: 10.1051/0004-6361/200811439

Astronomy & Astrophysics

Rotational mixing in massive binaries

Detached short-period systems

S. E. de Mink[1], M. Cantiello[1], N. Langer[1,2], O. R. Pols[1], I. Brott[1], and S.-Ch. Yoon[3]

[1] Astronomical Institute, Utrecht University, PO Box 80000, 3508 TA Utrecht, The Netherlands
e-mail: [S.E.deMink;M.Cantiello;N.Langer;O.R.pols;I.Brott]@uu.nl
[2] Argelander-Institut für Astronomie der Universität Bonn, Auf dem Hügel 71, 53121 Bonn, Germany
[3] Dep. of Astronomy & Astrophysics, Univ. of California, Santa Cruz, CA95064, USA
e-mail: scyoon@ucolick.org

Received 28 November 2008 / Accepted 2 February 2009

ABSTRACT

Models of rotating single stars can successfully account for a wide variety of observed stellar phenomena, such as the surface enhancements of N and He observed in massive main-sequence stars. However, recent observations have questioned the idea that rotational mixing is the main process responsible for the surface enhancements, emphasizing the need for a strong and conclusive test for rotational mixing.

We investigate the consequences of rotational mixing for massive main-sequence stars in short-period binaries. In these systems the tides are thought to spin up the stars to rapid rotation, synchronous with their orbital revolution. We use a state-of-the-art stellar evolution code including the effect of rotational mixing, tides, and magnetic fields. We adopt a rotational mixing efficiency that has been calibrated against observations of rotating stars under the assumption that rotational mixing is the main process responsible for the observed surface abundances.

We find that the primaries of massive close binaries ($M_1 \approx 20\ M_\odot$, $P_{\rm orb} \lesssim 3$ days) are expected to show significant enhancements in nitrogen (up to 0.6 dex in the Small Magellanic Cloud) for a significant fraction of their core hydrogen-burning lifetime. We propose using such systems to test the concept of rotational mixing. As these short-period binaries often show eclipses, their parameters can be determined with high accuracy.

For the primary stars of more massive and very close systems ($M_1 \approx 50\ M_\odot$, $P_{\rm orb} \lesssim 2$ days) we find that centrally produced helium is efficiently mixed throughout the envelope. The star remains blue and compact during the main sequence evolution and stays within its Roche lobe. It is the less massive star, in which the effects of rotational mixing are less pronounced, which fills its Roche lobe first, contrary to what standard binary evolution theory predicts. The primaries will appear as "Wolf-Rayet stars in disguise": core hydrogen-burning stars with strongly enhanced He and N at the surface. We propose that this evolution path provides an alternative channel for the formation of tight Wolf-Rayet binaries with a main-sequence companion and might explain massive black hole binaries such as the intriguing system M33 X-7.

Key words. binaries: close – stars: rotation – stars: abundances – Magellanic Clouds – stars: Wolf-Rayet – X-rays: binaries

1. Introduction

The rotation rate is considered as one of the main initial stellar parameters, along with mass and metallicity, which determine the fate of single stars. Rotation deforms the star to an oblate shape (of which Achernar is an extreme example, see Domiciano de Souza et al. 2003), it interplays with the mass loss from the star (e.g. Friend & Abbott 1986; Langer 1998; Maeder & Meynet 2000a) and it induces instabilities in the interior leading to turbulent mixing in otherwise stable layers (e.g. Meynet & Maeder 1997). As rotationally induced mixing can bring processed material from the core to the surface, it has been proposed as explanation for observed surface abundance anomalies, such as a nitrogen enrichment found in several massive main-sequence stars (e.g. Walborn 1976; Maeder & Meynet 2000b; Heger & Langer 2000). In models of rapidly rotating massive stars, rotational mixing can efficiently mix the centrally produced helium throughout the stellar envelope. Instead of expanding during core H burning as non-rotating models do, they stay compact, become more luminous and move blue-wards in the Hertzsprung-Russell diagram. This type of evolution is commonly referred to as (quasi-)chemically homogeneous evolution (Maeder 1987; Yoon & Langer 2005). Some over-luminous O and WNh[1] in the Magellanic Clouds in the Magellanic Clouds have been put forward as examples pf this type of evolution (Bouret et al. 2003; Walborn et al. 2004; Mokiem et al. 2007; Martins et al. 2008). This alternative evolutionary scenario has been proposed as a way to create rapidly rotating massive helium stars as the possible progenitors of long gamma-ray bursts within the collapsar scenario (Yoon & Langer 2005; Woosley & Heger 2006; Cantiello et al. 2007).

Multiple attempts have been made to constrain the efficiency of rotational mixing (e.g. Gies & Lambert 1992; Fliegner et al. 1996; Daflon et al. 2001; Venn et al. 2002; Korn et al. 2002; Huang & Gies 2006; Mendel et al. 2006), but often these attempts remained inconclusive due to limited sample sizes or a strong bias towards stars with low projected velocities. The VLT-FLAMES survey provided, for the first time, a large sample of massive stars with accurate abundance determinations,

[1] Wolf-Rayet stars with evidence of enhanced nitrogen and hydrogen in their spectra (e.g. Schnurr et al. 2008).

covering a wide range of projected rotational velocities (Evans et al. 2005; Hunter et al. 2008). This sample was used to calibrate the efficiency of rotational mixing, under the assumption that rotational mixing is the main process responsible for the observed enhancements (Brott et al. 2009).

These authors performed a population synthesis, based on detailed models of rotating single stars, to reproduce the properties of the VLT-FLAMES sample. They find that their models cannot account for a large number (20% of the sample) of highly nitrogen-enriched, slow rotators and a group of evolved fast rotators which are relatively non-enriched (a further 20% of the sample). This raises the question whether other processes play an important role in explaining the nitrogen enhancements of massive main-sequence stars, such as mass transfer in binaries (Langer et al. 2008).

Regardless of the successes of rotating stellar models to explain a variety of stellar phenomena (Maeder & Meynet 2000b), rotational mixing is still a matter of debate. Clearly a conclusive observational test for the concept of rotational mixing is needed. In this paper we propose to use eclipsing binaries for this purpose.

Eclipsing binaries have frequently been used to test stellar evolution models as they provide accurate stellar masses, radii and effective temperatures. Even beyond our own Galaxy, in the Magellanic Clouds, stellar parameters of O and early B stars have been determined with accuracies of 10% (Harries et al. 2003; Hilditch et al. 2005), which have been used to test binary evolution models (e.g. De Mink et al. 2007). As rotational mixing is more important in more massive stars (e.g. Heger et al. 2000), it is a major advantage to know the stellar masses for quantitative testing of the efficiency of rotational mixing.

In close binaries with orbital periods $P_{\rm orbit}$ less than a few days, the tides are so strong that the stars rotate synchronously with the orbital motion: $P_{\rm spin} = P_{\rm orbit}$. With stellar radii known from eclipse measurements, this enables us to determine the rotational velocity directly from the orbital period. This is the second important advantage of using binaries for testing rotational mixing with respect to single stars. For single stars fitting of spectral lines allows only for the determination of $v \sin i$, where v is the rotational velocity at the equator and i the inclination of the rotation axis, which is generally not known.

Here, we propose to use eclipsing binaries, consisting of two detached main-sequence stars. Detailed calculations of binary evolution show that if one of the stars fills its Roche lobe during the main sequence, it does not detach again before hydrogen is exhausted in the core, except maybe for a very short thermal timescale (Wellstein et al. 2001; De Mink et al. 2007). Turning this around we find that, in a binary with two detached main-sequence stars, we can safely exclude the occurrence of previous mass transfer. In other words, the fact that a system consists of two detached main-sequence stars, constrains the evolutionary history. In contrast, for a fast rotating apparently single star we do not know whether the star was born as a rapidly rotating single star, or whether the rapid rotation is the result of mass transfer in a binary or of a binary merger. The companion, if still present, may be very hard to detect, being a faint low-mass star in a wide orbit[2].

If the spectra of a binary are of high quality, one can determine the surface abundances of the two components (e.g. Leushin 1988; Pavlovski & Hensberge 2005; Rauw et al. 2005). These surface abundances, together with accurate determinations of the stellar parameters and the orbital period have the potential of strongly constraining the efficiency of rotational mixing.

The evolution of close massive binaries has been modeled by various groups (e.g. Podsiadlowski et al. 1992; Pols 1994; Wellstein et al. 2001; Wellstein & Langer 1999; Nelson & Eggleton 2001; Belczynski et al. 2002; Petrovic et al. 2005a; Vanbeveren et al. 2007; De Mink et al. 2007, and references therein). In this work we use a detailed binary evolution code to predict the surface abundances for massive detached close binaries. In addition we discuss models of very massive close binaries, in which rotational mixing can be so efficient that the change in chemical profile leads to changes in the stellar structure.

2. Stellar evolution code

We model the evolution of rotating massive stars using the 1D hydrodynamic stellar evolution code described by Yoon et al. (2006) and Petrovic et al. (2005b), which includes the effects of rotation on the stellar structure and the transport of angular momentum and chemical species via rotationally induced hydrodynamic instabilities (Heger et al. 2000). The rotational instabilities considered are: dynamical shear, secular shear, Eddington-Sweet circulation and the Goldreich-Schubert-Fricke instability (Heger et al. 2000). Two processes dominate rotational mixing in massive stars: Eddington-Sweet circulation, large-scale meridional currents resulting from the thermal imbalance between pole and equator characteristic of rotating stars (von Zeipel 1924; Eddington 1925, 1926; Vogt 1925) and shear mixing, eddies, that can form between two layers of the star rotating at different angular velocity (e.g. Zahn 1974). We take into account angular momentum transport by magnetic torques as proposed by Spruit (2002) as these can successfully provide the coupling between the stellar core and envelope necessary to explain the observed spins in young compact stellar remnants (Heger et al. 2005; Petrovic et al. 2005b; Suijs et al. 2008).

Mixing of chemical species and the transport of angular momentum are implemented as diffusion processes. For convection we assume a mixing length parameter $\alpha_{\rm MLT} = 1.5$. In semi-convective regions we assume efficient mixing ($\alpha_{\rm SEM} = 1.0$, as defined in Langer 1991). The turbulent viscosity is determined as the sum of the convective and semi-convective diffusion coefficients and those that arise from the rotationally induced instabilities. The inhibiting effect of gradients in the mean molecular weight on rotational mixing is decreased by a factor $f_\mu = 0.1$ (Yoon et al. 2006).

Brott et al. (2009) calibrated the efficiency of rotationally induced mixing using data from the VLT-FLAMES survey of massive stars, assuming that rotational mixing is the main process responsible for the observed enhancements. To reproduce the extension of the main sequence in the Hertzsprung-Russell diagram, they assumed overshooting of 0.355 times the pressure scale height. The main parameter responsible for the efficiency of rotational mixing is $f_{\rm c}$, defined as the contribution of rotationally induced instabilities to the diffusion of chemical species (Heger et al. 2000). Brott et al. (2009) found that $f_{\rm c} = 0.0228$ is needed to reproduce the spread in N abundances observed in the VLT-FLAMES data (Hunter et al. 2008). We do not consider possible mixing by instabilities related to magnetic buoyancy due to winding up of the magnetic field lines through differential rotation (Spruit 2002) as this leads to too efficient mixing (Hunter et al. 2008).

[2] Abundance determinations of boron, if available, may be used to distinguish between binary effects and pure rotational mixing, see Fliegner et al. (1996).

Metallicity-dependent mass loss in the form of stellar winds has been included as in Yoon et al. (2006); Brott et al. (2009). For the associated angular momentum loss we assume that mass is lost with the specific angular momentum equal to the latitudinally averaged specific angular momentum of the surface layer. The mass loss is thus assumed to be independent of latitude.

The effect of mass and angular momentum loss on the binary orbit is computed according to Podsiadlowski et al. (1992), with the specific angular momentum of the wind calculated according to Brookshaw & Tavani (1993). We assume that the orbit is circular and that the spins of the stars are perpendicular to the orbital plane. Tidal interaction is modeled as described in Detmers et al. (2008) using the timescale for synchronization by turbulent viscosity (Zahn 1977), see also Sect. 3. Angular momentum is transported between the surface layers and the inner regions by magnetic torques and rotational instabilities. At the onset of central H burning, we assume that the rotation of the stars is rigid and synchronized with the orbital motion.

Initial composition

We discuss single stellar models starting with three different initial compositions, representing the composition of the Small and Large Magellanic Cloud (abbreviated as SMC and LMC) and the Galaxy (GAL) following the approach by Brott et al. (2009) to which we refer for details. For C, O, Mg and Si we use the average abundances determined for stars in the VLT-FLAMES survey (Hunter et al. 2007). For the Magellanic Clouds we adopt the N abundance measured for HII regions which is in agreement with the lowest observed N abundances in the VLT-FLAMES sample (Hunter et al. 2007, and references therein). For the remaining heavy elements we adopt solar abundances by Asplund et al. (2005) scaled down by 0.7 dex for the SMC and 0.4 dex for the LMC. For our binary models we have assumed the SMC composition. The opacity tables of OPAL (Iglesias & Rogers 1996) are adopted, where the Fe abundance is used to interpolate between the tables of different metallicity.

3. Stellar rotation under the influence of tides

In a close binary, angular momentum and kinetic energy can be exchanged between the two stars and their orbit through tides. The system tends to evolve towards a state of minimum mechanical energy due to dissipative processes. This is an equilibrium state, where the orbit is circular, the spins of the stars are aligned and perpendicular to the orbital plane and the stars are in synchronous rotation with the orbital motion, such that $P_{\rm spin} = P_{\rm orbit}$. How quickly this equilibrium state is approached depends on the efficiency of the processes responsible for the energy dissipation.

The most efficient form of energy dissipation takes place in turbulent regions of the star, such as convective layers, where the kinetic energy of the large-scale flow induced by the tides cascades down to smaller and smaller scales, until it is dissipated into heat. Zahn (1977, 1989) estimated the timescale for synchronization due to this "turbulent viscosity" as a function of the ratio q of the mass of the companion star to the mass of the star under consideration and on the ratio of the stellar radius R over the separation a between the two stars:

$$\tau_{\rm sync,\,turb} = f_{\rm turb}\, q^{-2} \left(\frac{R}{a}\right)^{-6} \text{ year}. \quad (1)$$

The proportionality factor $f_{\rm turb}$ depends on the structure of the star, on the location of the turbulent layers and on the timescale for dissipation of kinetic energy, which is uncertain. Nevertheless, the dependence of the time scale on R/a is so steep that, approximating $f_{\rm turb} \approx 1$, Zahn (1977) showed that this expression adequately explains the observed orbital period below which tides lead to synchronization.

In the absence of turbulent viscosity, another dissipative process is required in order to have efficient tides. If the star does not rotate synchronously, it experiences a varying gravitational potential, which triggers a large range of oscillations in the star. These oscillations are damped near the stellar surface by radiative dissipation. Zahn (1975) derived the corresponding timescale for synchronization:

$$\tau_{\rm sync,\,rad} = f_{\rm rad}\, q^{-2}\,(1+q)^{-5/6} \left(\frac{R}{a}\right)^{-17/2} \text{ year}, \quad (2)$$

$$\text{where } f_{\rm rad} = 52^{-5/3}\, E_2 \left(\frac{I}{MR^2}\right) \left(\frac{GM}{R^3}\right)^{-1/2}.$$

Here, M denotes the mass of the star under consideration, I its moment of inertia and E_2 the tidal coefficient, which is sensitive to the structure of the star, in particular to the size of the convective core: $E_2 \propto (R_{\rm core}/R)^8$ (Zahn 1977).

The early-type massive stars considered in this work have radiative envelopes (except for convective zones just below the surface which contain almost no mass, e.g. Cantiello et al. 2009) and synchronization by radiative damping has been proposed to be the most efficient dissipation mechanism. However, in fast rotating stars turbulence is induced by rotational instabilities and one may argue that the first timescale applies also to these stars (Toledano et al. 2007). In addition Witte & Savonije (1999) show that in some cases resonance locking can contribute to even more efficient tidal dissipation.

In Fig. 1 we compare both synchronization timescales with the main-sequence lifetime of the more massive star in a binary. For this plot we have used the radii of non-rotating zero-age main sequence stars assuming a metallicity of $Z = 0.004$ and a mass ratio of $M_2/M_1 = 0.75$. For E_2 we use an analytic approximation by Hurley et al. (2002), for the Roche-lobe radius we use the analytic expression by Eggleton (1983). The diagram shows that in binaries with orbital periods shorter than approximately 3–5 days, the timescale for synchronization is less than one percent of the main-sequence lifetime $\tau_{\rm MS}$, regardless of the actual process responsible for the synchronization. The resulting equatorial velocity of the primary star, assuming synchronous rotation, is given in km s^{-1} along contour lines.

For comparison: the average equatorial velocity for apparently single stars in the VLT-FLAMES survey with masses between 7 and 25 $M_\odot$ is 150 km s^{-1} for the LMC and 175 km s^{-1} for the SMC (Hunter et al. 2008). In most binaries tides will slow down the rotation of the star, but in the tightest binaries the rotation rate is higher than that for average single stars. Note that the binary systems of interest in this work, for which the components have high enough equatorial velocities to show significant surface abundance changes by rotational mixing ($\gtrsim$100–150 km s^{-1}, see Sect. 4), are in the region where tides are very efficient, according to both prescriptions for the synchronization timescale.

4. Rotational mixing in single star models

Any element produced or destroyed in the hot interior of the star can in principle be used as a tracer of rotational mixing. The amount by which the surface abundance of a particular element

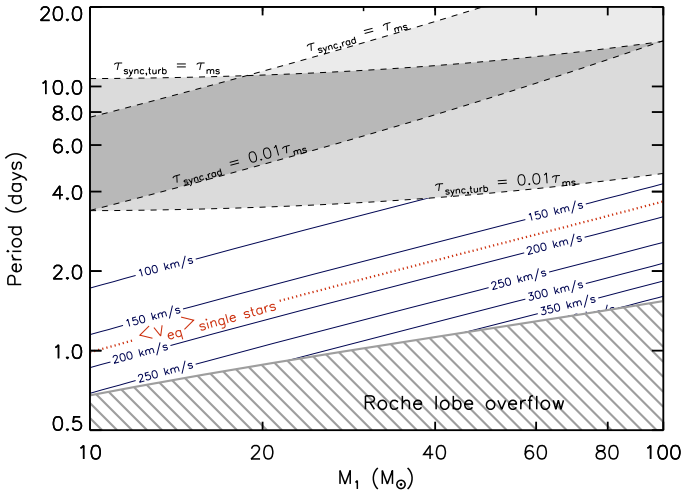

Fig. 1. Timescales for tidal synchronization. The four dashed lines indicate where the timescales for tidal synchronization by turbulent viscosity $\tau_{\rm sync,\,turb}$ and radiative dissipation $\tau_{\rm sync,\,rad}$ for zero-age main-sequence stars are equal to (one percent of) the main-sequence lifetime $\tau_{\rm ms}$ of the most massive star of a binary system, see Sect. 3 for details. In the region below the gray-shaded bands, tides quickly synchronize the stellar rotation with the orbit. The resulting equatorial velocity in km s^{-1} for the primary star is indicated with contour levels, assuming the radius at the onset of hydrogen burning. We have assumed a metallicity of $Z = 0.004$ and a mass ratio $M_2/M_1 = 0.75$, to be consistent with the models presented in Sect. 4. The average velocity measured for apparently single stars in the SMC, $\langle v_{\rm eq}\rangle = 175$ km s^{-1}, is plotted with a dotted line. Very short orbital periods are excluded (hashed region) as the stars fill their Roche lobe at zero-age.

changes depends on the location in the star where the element is processed.

Helium is the most important element synthesized during core hydrogen burning. By the time a substantial amount of helium has been formed in the stellar core, a gradient in mean molecular weight has been established at the interface between the core and the envelope, which has an inhibiting effect on rotationally induced mixing. Models of moderately fast rotating stars (with an equatorial velocity of about 170 km s^{-1} and a mass of about 20 $M_\odot$) show that helium will only appear at the surface towards the very end of the main-sequence evolution. In more massive stars, the helium surface abundance may be significantly enhanced but this is partly due to the strong stellar winds. This makes helium not very suitable for testing the effect of rotational mixing.

A better tracer for rotational mixing during the main-sequence evolution is nitrogen, which is produced in the hot interior layers on a very short time scale when carbon is converted into nitrogen by CN-cycling. On a longer timescale (about 1–2 Myr in the center of a 20 $M_\odot$ star) the CNO cycle comes into equilibrium, leading to additional N at the expense of both carbon and oxygen. Rotational mixing can bring nitrogen to the surface, resulting in a gradual increase of the nitrogen surface abundance over the main-sequence lifetime (Fig. 2). Nitrogen can be measured in rotating B-type stars in the Magellanic Clouds with accuracies of 0.2–0.25 dex (Hunter et al. 2008). Carbon decreases accordingly, but cannot be measured as accurately and is therefore less suitable as a tracer of rotational mixing. Other elements such as boron can be used, but these are less abundant and may be hard to detect, especially in metal-poor environments such as the Magellanic Clouds.

Rotational mixing becomes more efficient in higher-mass stars since radiation pressure becomes more important, which helps to overcome the entropy barrier at the interface between the core and the envelope. Also, the ratio of the timescale for meridional circulation with respect to the main-sequence lifetime decreases with increasing mass (Yoon et al. 2006). The disadvantage of using very massive stars as test cases for rotational mixing is the uncertainty in their mass-loss rates. As mass loss exposes deeper layers of the star, enriched in N and He, it has qualitatively the same effect on the surface composition as rotational mixing. At lower metallicity mass loss in the form of a radiatively driven stellar wind is reduced. Therefore, also the uncertainty in the mass-loss rate is less important.

Figure 2 shows the nitrogen surface abundance as a function of time for rotating single stellar models of 20 $M_\odot$ with three different initial compositions, representative for the relatively metal-poor composition of the Small and Large Magellanic Cloud, and for a mixture representing stars in the Galaxy. The equilibrium abundances for N in the center for CN- and CNO-cycling are plotted as horizontal lines. The Galactic model with an equatorial velocity of 230 km s^{-1} shows nitrogen enhancements up to about 0.3 dex, while in the SMC model the N abundance increases by up to approximately 0.8 dex. The high C/N ratio in the Magellanic Clouds is partly responsible for this effect as it leads to a strong increase of N during CN-cycling (Brott et al. 2009). Indeed, in the VLT-FLAMES survey, Hunter et al. (2008) find a larger spread in N abundances for the stars in the Magellanic Clouds than for ones in the Galactic stars. We conclude that the Magellanic Clouds are the most promising location for testing rotational mixing, as the effect of rotational mixing is most pronounced in the N surface abundances.

5. Binary models

In this section we present binary evolution models calculated with the same set of input physics as the single stellar models presented in Sect. 4, taking into account the effects of mass and angular momentum loss on the orbit and spin-orbit coupling by tides. We assume a composition representative of the Small Magellanic Cloud, which is relatively metal-poor and has a high carbon to nitrogen ratio. We discuss two specific model sets: systems with a massive primary, $M_1 = 20\ M_\odot$, in Sect. 5.1 and systems with a very massive primary, $M_1 = 50\ M_\odot$, in Sect. 5.2.

5.1. Massive binaries (20 $M_\odot$ + 15 $M_\odot$)

With the Small Magellanic Cloud sample of double-lined eclipsing binaries by Harries et al. (2003) and Hilditch et al. (2005) in mind, which contains 21 detached systems[3] with orbital periods ranging from 1–4 days and primary masses ranging from 7–23 $M_\odot$, we chose to model the following binary systems. For the mass of the primary component we adopt 20 $M_\odot$, for the secondary component 15 $M_\odot$. The evolution of both stars is followed starting at the onset of central hydrogen burning, at $t = 0$, until the primary star fills its Roche lobe, at $t = t_{\rm RL}$. We adopt orbital periods up to 3 days. In these systems the tides are efficient enough to keep both stars in synchronous rotation with the orbit (Sect. 3).

[3] Possibly only 20 systems are detached. For two of the systems an alternative semi-detached solution exists. For one of these systems a comparison to binary evolution models including the effects of mass transfer showed that the semi-detached solution was more consistent than the detached solution (De Mink et al. 2007).

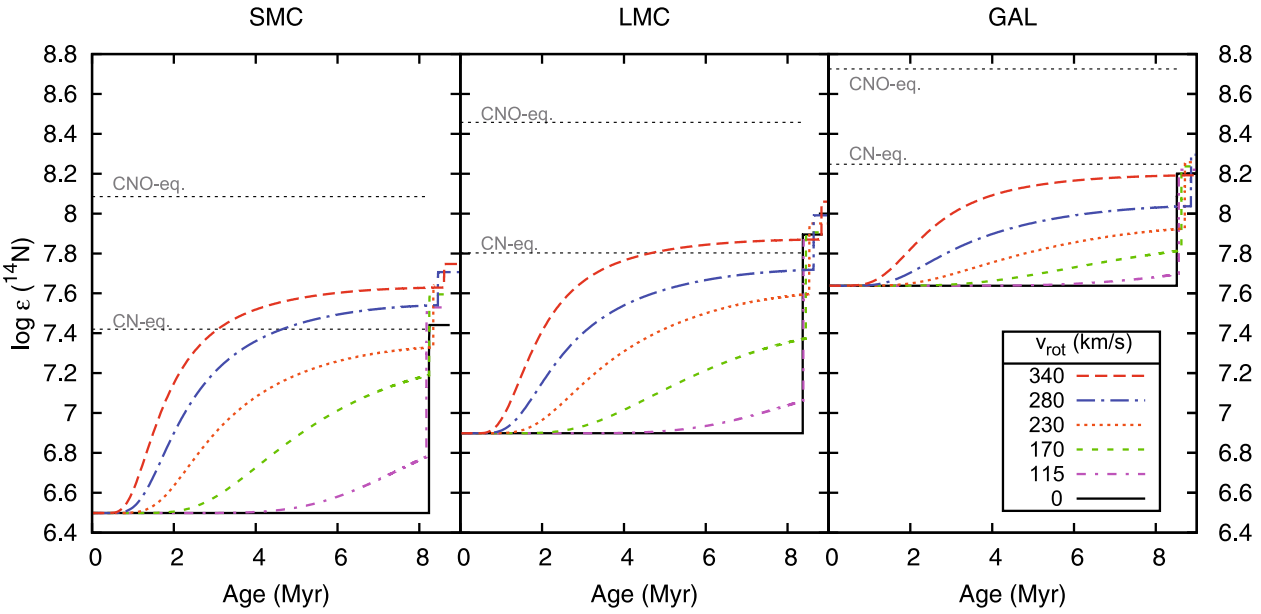

Fig. 2. Surface nitrogen abundance versus time for single stellar models of 20 $M_\odot$ with different (approximate) initial equatorial rotational velocities starting with the initial composition of the SMC (*left panel*), LMC (*center panel*) and GAL (*right panel*). The nitrogen abundance is given in the conventional units: the logarithm of the number fraction of nitrogen n_N with respect to hydrogen n_H, where the hydrogen abundance is fixed at 10^{12}, i.e. $\log \epsilon(N) = \log_{10}[n_N/n_H] + 12$.

Table 1. Key properties of the massive binary evolution models (20 $M_\odot$ + 15 $M_\odot$) as defined and discussed in Sect. 5.1.

P_{orb} (d)	t_{RL} (Myr)	t_{delay} (Myr)	$t_{RL} - t_{enh}$ (Myr)	R/R_{RL} ($t = t_{enh}$)	$X_{He,center}$ ($t = t_{RL}$)	$\log \epsilon(N^{14})$ ($t = t_{RL}$)	B_{RL}/B^a_{init}	C_{RL}/C^a_{init}	N_{RL}/N^a_{init}	$\langle v_{eq}\rangle^b$ (km s^{-1})	$v^b_{eq,RL}$ (km s^{-1})
1.1	3.3	1.3	1.0	0.92	0.42	7.12	0.11	0.87	4.17	243	267
1.2	3.9	1.6	1.2	0.90	0.47	7.07	0.08	0.85	3.71	228	260
1.4	5.0	2.1	1.5	0.86	0.55	6.98	0.06	0.82	3.04	203	248
1.6	5.5	2.7	1.0	0.86	0.61	6.89	0.07	0.83	2.45	181	234
1.8	6.0	3.2	0.9	0.86	0.65	6.85	0.07	0.83	2.27	166	228
2.0	6.3	3.7	0.6	0.87	0.69	6.81	0.09	0.86	2.05	152	216
2.2	6.7	4.1	0.5	0.89	0.73	6.79	0.10	0.87	1.96	141	212
2.4	6.9	4.5	0.4	0.90	0.75	6.77	0.11	0.88	1.87	131	207
2.6	7.1	4.9	0.2	0.93	0.78	6.74	0.13	0.90	1.74	123	199
2.8	7.2	5.2	0.1	0.96	0.79	6.73	0.14	0.91	1.69	116	196
3.0	7.3	5.6	0.0	0.99	0.81	6.70	0.15	0.92	1.59	110	190

[a] The surface mass fraction at the onset of Roche-lobe overflow divided by the initial mass fraction of resp. boron ($^{10}B + {}^{11}B$), carbon (^{12}C) and nitrogen (^{14}N).
[b] The equatorial rotational velocity for the primary star, averaged over time from the onset of hydrogen burning until the start of mass transfer (one before last column) and at the onset of Roche-lobe overflow (last column).

Surface abundances

The abundances of nitrogen, carbon, helium and boron at the surface of the primary star are shown as a function of time in Fig. 3, see also Table 1. The nitrogen abundances at the surface starts to increase after about 1 Myr for the 1.1 day binary, and after about 5 Myr for the 3.0 day binary. This time delay t_{delay} is the time it takes to transport the nitrogen from the deeper layers, where it is produced, to the surface[4]. The largest enhancement, 0.6 dex, is achieved in the 1.1 day binary. The shorter the orbital period, the faster the rotation of the stars, the more efficient rotational mixing and the faster the surface abundances change with time. On the other hand in the systems with short orbital periods the stars fill their Roche lobe at an earlier stage, leaving less time to modify their surface abundances.

The typical uncertainty in the nitrogen abundance determinations for stars in the VLT-FLAMES survey is about 0.2 dex. Therefore, to be able to detect whether nitrogen is enhanced, it should exceed the initial nitrogen abundance by 0.2 dex. The age at which this lower limit for detecting a surface nitrogen enhancement is exceeded is denoted as t_{enh} in Table 1. Systems with orbital periods shorter than 3 days all reach surface enhancements of 0.2 dex, at the latest just before they fill their Roche lobe. The time span during which the primary can be observed with a surface nitrogen abundance exceeding 6.7 dex, listed as $t_{RL} - t_{enh}$ in Table 1, is highest for the 1.4 day system, 1.5 Myr. For detached tidally locked main-sequence binaries with initial orbital periods greater than about 3 days we do not expect detectable N enhancements on the basis of these

[4] We define t_{delay} as the age at which the surface nitrogen abundance is enhanced by 0.01 dex.

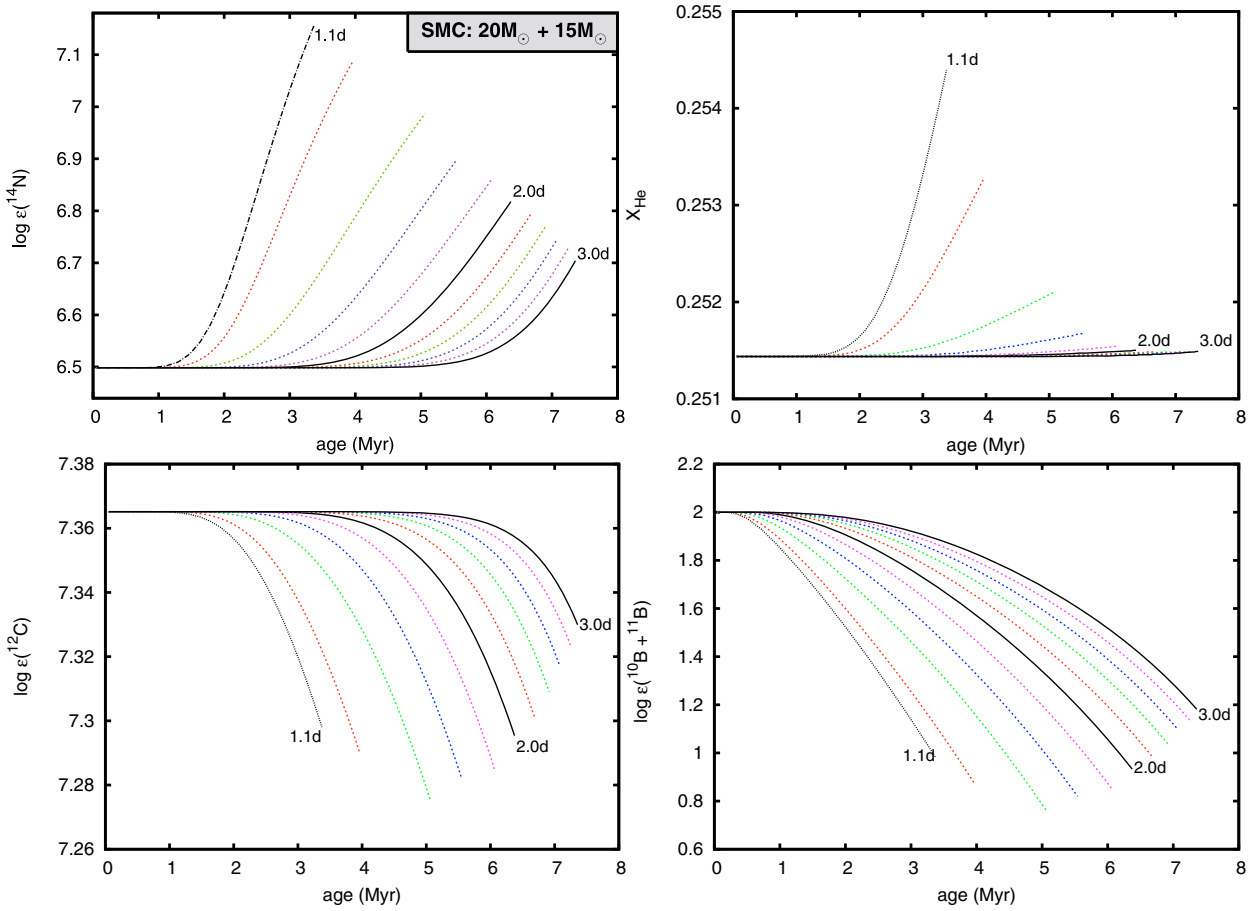

Fig. 3. Surface abundances of nitrogen (^{14}N), carbon (^{12}C), boron (^{10}B + ^{11}B) and the mass fraction of helium at the surface versus time for a 20 $M_\odot$ star with a 15 $M_\odot$ close companion. Note the different vertical scales. The abundance of an element X is given relative to hydrogen in the conventional units: $\log \epsilon(\mathrm{X}) = \log_{10}(n_\mathrm{X}/n_\mathrm{H}) + 12$, where n_X and n_H refer to the number fractions. The different lines show the evolution assuming initial orbital periods of 1.1 days and between 1.2 and 3 days, with a spacing of 0.2 days. The tracks are plotted from the onset of central H burning until the onset of Roche-lobe overflow. See also Table 1.

models: their rotation rates and therefore the efficiency of rotational mixing is too low.

While the nitrogen abundance increases, the carbon abundance decreases accordingly, see Fig. 3. It decreases by less than 0.1 dex in our models. The changes in the mass fraction of helium at the surface are very small, just over 1% at maximum for the tightest system. An element that is a very sensitive tracer of rotational mixing is boron. It is easily destroyed in the hotter layers just below the surface. Therefore the time delay for boron, after which the boron surface abundance starts to change, is very short. The change in the boron surface abundance is considerable, up to 1.2 dex in the 1.4 day model. In practice it may be hard to measure boron due to its low overall abundance.

The closer the stars are to filling their Roche lobe, the higher is their surface N abundance. This can be turned around and may be used to predict which binary systems are likely to show nitrogen surface enhancements. In Table 1 we indicate the Roche-lobe filling factor R/R_RL, defined as the radius of the primary star over the Roche-lobe radius, at the moment when the surface N enhancement exceeds the initial abundance by 0.2 dex. Based on these models, we predict that the observed systems with masses close to 20 and 15 $M_\odot$ have to fill their Roche lobes by about 86% or more before they show detectable surface N enhancements (see Table 1 Col. 5). We do note that the radii predicted by our models are sensitive to the assumed amount of overshooting.

In the last two columns of Table 1 we indicate the rotational velocity at the equator, averaged over time and at the onset of Roche-lobe overflow. Whereas a single star at this metallicity slows down its rotation rate due to its evolutionary expansion, the spin periods of the stars in tidally locked binaries are nearly constant because the orbit acts as an angular momentum reservoir. Therefore rotationally induced mixing is more important in a star in a tidally locked binary than in a single star that started with the same initial rotation rate. The effect is small, however, as the expansion mainly takes place after about 5–6 Myr for a 20 $M_\odot$ star. Binaries with orbital periods shorter than 2 days fill their Roche lobe before the expansion sets in. The effect is stronger at higher metallicity, where angular momentum loss by the stellar wind becomes important, see Sect. 6.

Expected trends with system mass and mass ratio

For an ideal comparison between models and observations one would prefer a model in which the binary parameters match the observed parameters. In the above, we discussed models with a specific choice for the primary mass and mass ratio and we only varied the initial orbital period. Here we discuss how our findings are expected to change for systems with slightly different system masses and mass ratios.

In more massive binaries rotational mixing is more efficient, such that they will show a shorter time delay, even

when measured in units of the core hydrogen-burning lifetime. Detectable surface enhancements are expected to occur at an earlier stage, while the stars are further away from filling their Roche lobe. At very high masses additional effects can play a role, which are discussed in Sect. 5.2. The secondary star in the models discussed above does not show significant surface abundance changes for C, N and He. The surface boron abundance does decrease by up to 0.6 dex for the 1.4 day model. In systems with mass ratios closer to 1, the time scale for rotational mixing becomes similar in both stars and nitrogen enhancements are expected for both stars.

Another effect of changing the mass ratio is that the size of the Roche lobe changes. A more extreme mass ratio results in a wider Roche lobe for the primary, if the primary mass and orbital period are kept constant. The efficiency of rotational mixing does not change, as it depends on the rotational period which is fixed by the orbital period. However, the star has more space to expand before it fills its Roche lobe. We noted above that the primary stars fill their Roche lobes by at least 86% before they show detectable surface N enhancements (see also Sect. 6). This changes to approximately 83% and 76% for mass ratios of $q = 0.5$ and $q = 0.25$ respectively. A bigger Roche lobe also leaves more time to enhance the surface abundance. This implies a greater chance of catching the system in a stage where the surface abundance is significantly enhanced.

To summarize: the biggest surface N enhancements are expected for systems with a high-mass primary, which is close to filling its Roche lobe, with a companion which has a significantly lower mass in an orbit of no more than a few days.

5.2. Very massive binaries (50 $M_\odot$ + 25 $M_\odot$)

In more massive binaries, rotational mixing can be so efficient that the change in chemical profile leads to significant structural changes. In this model set we adopt a primary mass of 50 $M_\odot$, a secondary mass of 25 $M_\odot$ and orbital periods varying from 1.5 to 4 days, assuming an SMC composition to be consistent with the models presented in Sect. 5.1. Although such massive close systems are rare, observational counterparts do exist, for example two of the four massive binaries presented by Massey et al. (2002) which are located in the R136 cluster at the center of the 30 Doradus nebula in the Large Magellanic Cloud: R136-38[5] and R136-42[6]. Another example with an even closer orbit is [L72] LH 54-425[7] located in the LH 54 OB association in the Large Magellanic Cloud (Williams et al. 2008). All three binary systems have O-type main-sequence components, which reside well within their Roche lobes.

Figure 4 shows the evolution of the primary stars in the Hertzsprung-Russell diagram, until one of the stars in the binary fills its Roche lobe (not necessarily the primary, see below). At the onset of hydrogen burning their location in the diagram is very similar, although the stars in tighter binaries, which rotate faster, are slightly cooler and bigger: a direct consequence of the centrifugal force. As they evolve their tracks start to deviate. The wider systems ($P_{\rm orb} > 2.0$ d) evolve similarly to non-rotating stars: they expand during core hydrogen burning, evolving towards cooler temperatures until they fill their Roche lobe. Their evolutionary tracks overlap in the Hertzsprung-Russell diagram.

The primaries in the tighter systems ($P_{\rm orb} < 2.0$ d) behave very differently: they evolve left- and up-ward in the HR-diagram, becoming hotter and more luminous while they stay relatively compact. The transition in the morphology of the tracks around $P_{\rm orb} \approx 2$ days is similar to the bifurcation found for fast rotating single stars (Maeder 1987; Yoon & Langer 2005).

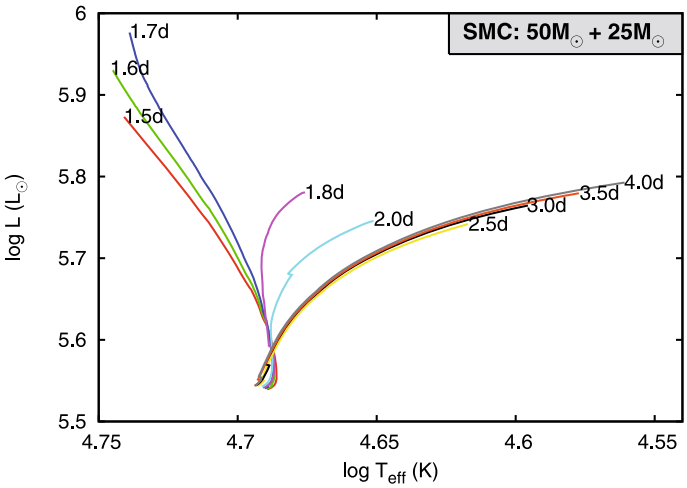

Fig. 4. The evolution from the onset of central H burning until the moment of Roche-lobe overflow for a 50 $M_\odot$ star in a binary with a 25 $M_\odot$ companion (not plotted) with initial orbital periods between 1.5 and 4 days.

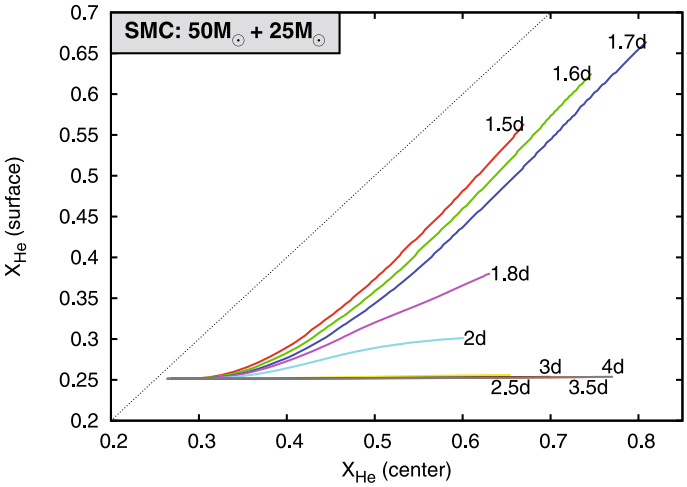

Fig. 5. Helium abundance at the surface as a function of the helium abundance in the center for the same systems as plotted in Fig. 4.

Surface abundances

Rotational mixing is so efficient in these systems that even a large amount of helium can be transported to the surface. Figure 5 depicts the helium mass fraction at the surface as a function of the helium mass fraction in the center. In the hypothetical case that mixing would be extremely efficient throughout the whole star, the surface helium abundance would be equal to the central helium abundance at all time. This is indicated by the dotted line. For the widest systems, the surface helium mass fraction is not affected by rotational mixing at all, while for the tighter systems $X_{\rm He}$ reaches up to 65%. They follow the evolution of chemically homogeneous stars. Figure 5 also shows that for each system, mass transfer starts before all hydrogen is converted into helium in the center. Note that the highest central He mass fraction when mass transfer starts is reached in the 1.7 day

[5] $M_1 = 56.9 \pm 0.6\ M_\odot$, $M_2 = 23.4 \pm 0.2\ M_\odot$ and $P_{\rm orb} = 3.39$ d.
[6] $M_1 = 40.3 \pm 0.1\ M_\odot$, $M_2 = 32.6 \pm 0.1\ M_\odot$ and $P_{\rm orb} = 2.89$ d.
[7] $M_1 = 47 \pm 2\ M_\odot$, $M_2 = 28 \pm 1\ M_\odot$ and $P_{\rm orb} = 2.25$ d.

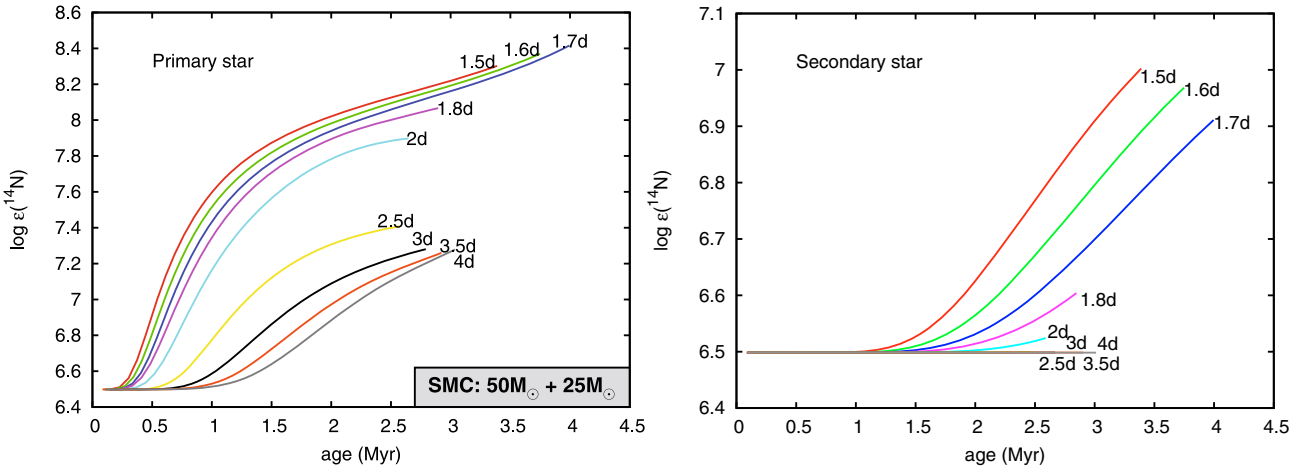

Fig. 6. Nitrogen abundance as a function of age at the surface for the primary and secondary star of the same systems as plotted in Fig. 4. Note the different scales.

Table 2. Key properties of very massive binaries (50 $M_\odot$+ 25 $M_\odot$) as described in Sect. 5.2 (see also Table 1 and Sect. 5.1). In the last column we indicate which component fills its Roche lobe first.

$P_{\rm orb}(d)$	$t_{\rm RL}$(Myr)	$X_{\rm He,\,center}$	$X_{\rm He,\,surface}$	log $\epsilon(N^{14})$	$B_{\rm RL}/B_{\rm init}$	$C_{\rm RL}/C_{\rm init}$	$N_{\rm RL}/N_{\rm init}$	$\langle v_{\rm eq}\rangle$ (km s^{-1})	$v_{\rm eq,\,RL}$ (km s^{-1})	RLOF
1.5	3.4	0.68	0.56	8.30	2.0×10^{-6}	9.0×10^{-2}	37	304	315	Sec.
1.6	3.7	0.75	0.63	8.37	6.6×10^{-7}	9.1×10^{-2}	37	289	307	Sec.
1.7	4.0	0.81	0.66	8.41	4.7×10^{-7}	9.5×10^{-2}	37	277	310	Sec.
1.8	2.9	0.64	0.38	8.06	2.8×10^{-4}	2.3×10^{-1}	30	262	315	Prim.
2.0	2.6	0.61	0.30	7.90	2.4×10^{-3}	4.0×10^{-1}	23	240	305	Prim.
2.5	2.6	0.66	0.26	7.41	8.1×10^{-3}	7.4×10^{-1}	8.0	200	279	Prim.
3.0	2.8	0.71	0.25	7.28	1.3×10^{-2}	7.8×10^{-1}	6.0	172	261	Prim.
3.5	2.9	0.75	0.25	7.26	1.8×10^{-2}	8.0×10^{-1}	5.7	152	248	Prim.
4.0	3.0	0.78	0.25	7.27	2.4×10^{-2}	7.9×10^{-1}	6.0	137	236	Prim.

system (more than 80%), whereas on the basis of standard binary evolution theory (e.g. Kippenhahn & Weigert 1967) one would expect this to occur in the widest system. This anomalous behavior is connected to the evolution of the radius, as discussed below.

All systems show big enhancements of nitrogen at the surface of the primary, see Fig. 6. The wider systems are enhanced by up to 0.9 dex. In the tight systems the enhancement reaches almost 2 dex. This extreme increase is partly due to the fact that abundance is measured relative to hydrogen, which is significantly depleted at the surface of the primaries in the tightest systems (cf. Table 2). Also the secondary stars show nitrogen surface enhancements, of up to 0.5 dex.

Evolution of the radius

The increase of helium in the envelopes of the primary stars in the tightest binaries leads to a decrease of the opacity and an increase in mean molecular weight in the outer layers, resulting in more luminous and more compact stars. In Fig. 7 we plot the stellar radii as a fraction of their Roche-lobe radii. The primary stars in the wider systems expand and fill their Roche lobe after about 2.5–3 Myr. Contrary to what one might expect, we find that Roche-lobe overflow is delayed in tighter binaries. Whereas classical binary evolution theory predicts that the primary star is the first to fill its Roche lobe, we find instead that for systems with $P_{\rm orb} \leq 1.7$ days it is the less massive secondary star that starts to transfer mass towards the primary. During this phase of reverse mass transfer from the less massive to the more massive star, the orbit widens. Nevertheless we find that, if we continue our calculations, the two stars come into contact shortly after the onset of mass transfer and the stars are likely to merge.

Expected trends with system mass and mass ratio

In more massive systems the effect of rotational mixing becomes stronger in both components. This may allow for chemically homogeneous evolution to occur in binary systems with wider orbits. If the mass ratio is closer to one, $M_2 \approx M_1$, the effect of rotational mixing becomes comparable in both stars, and they may both evolve along an almost chemically homogeneous evolution track. In that case both stars can stay within their Roche lobe and gradually become two compact WR stars in a tight orbit. In a system with a more extreme mass ratio, $M_2 \ll M_1$, the secondary star will hardly evolve or expand during the core hydrogen-burning lifetime of the primary. Also in this case Roche-lobe overflow may be avoided during the core hydrogen-burning lifetime of the primary component, leading to the formation of a Wolf-Rayet star with a main-sequence companion in a tight orbit. The parameter space in which this type of evolution can occur will be examined in a subsequent paper.

6. Discussion

We have shown that rotational mixing can have important effects in close massive binaries. The mixing parameters in our code have been calibrated against observations of rotating massive stars in the VLT-FLAMES survey under the assumption that rotational mixing is the main process responsible for the observed surface N enhancements (see Sect. 2). The predictions

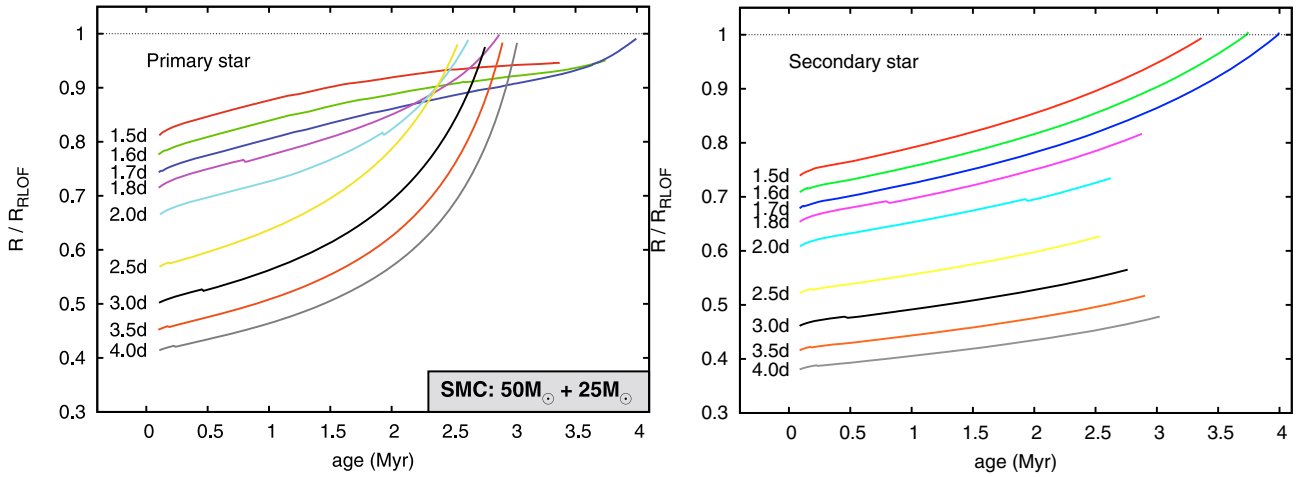

Fig. 7. Radius as fraction of the Roche-lobe radius for the primary (*left panel*) and secondary star (*right panel*) of the same systems as plotted in Fig. 4.

we present for close binaries can be used to test the validity of this assumption.

In Sect. 4 we conclude that eclipsing binaries in the Magellanic Clouds are the most promising test cases for rotational mixing. In these systems we expect the biggest enhancements of N at the surface. Also, the uncertainty in the mass-loss rates plays a less important role, as radiatively driven winds are reduced at low metallicity. A disadvantage of Magellanic Cloud binaries with respect to Galactic systems is the greater distance. Long integration times may be needed to obtain spectra with high enough quality to determine the stellar parameters and abundances. The advantage of using eclipsing binaries is that we can compare directly to evolution models with corresponding masses and orbital periods. Therefore, just a few well-studied systems may be enough to put constraints on the efficiency of rotational mixing. However, ideally one would prefer a large sample to enable a statistical comparison.

The main parameter in our code that affects the efficiency of mixing due to rotational instabilities is f_c (see Sect. 2) which has been calibrated directly against the surface N abundances in the VLT-FLAMES survey. However, the calibration involves multiple parameters, such as f_μ which is a measure of how effectively a gradient in mean molecular weight can inhibit rotational mixing. We expect that uncertainties in this parameter are not important for our predictions for nitrogen, as this element is mainly produced and transported to the envelope early in the evolution, before a strong mean molecular-weight gradient has been established at the interface between the core and the envelope. However, a lower value of f_μ may lead to higher helium surface abundances, which may facilitate the possibility of chemically homogeneous evolution in close binaries, but this remains to be investigated.

We use a large amount of overshooting in our models (0.355 times the pressure scale height H_p), to reproduce the extension of the main sequence observed in the VLT-FLAMES data. However, the amount of overshooting is an uncertain parameter and some authors quote lower values for the amount of overshooting, for example Schroder et al. (1997) who find 0.24–0.32H_p based on eclipsing binaries with stellar masses between 2.5 and 6.5 $M_\odot$, (see also Stothers & Chin 1992; Alongi et al. 1993). We recomputed one of our models (20 + 15 $M_\odot$, 3 days) without overshooting we find that, although the stars are less luminous as expected, the surface nitrogen abundance and the radius at a given time are very similar (deviations of less 0.01 dex in the N abundance at a given age, and less than 4% in the radius for a given nitrogen surface abundance). For tighter binaries we expect an even smaller effect on the radius. We conclude that our predictions are not very sensitive to the uncertainties in the overshooting parameter.

In our models we assume that mixing processes in binaries operate in the same way as in single stars. For both single stars and binary members we find that the stellar interior rotates nearly rigidly (at least during the early phase of evolution of interest here) as a result of efficient internal angular momentum transport by magnetic torques. Having very similar internal rotational profiles, the only difference in our models arises from the evolution of the rotation rate, which in single stars is governed by angular momentum loss and evolutionary expansion, while in binaries the tides play a major role. However, in the binary models we consider the stars are close to filling their Roche lobe. They are slightly deformed in a lob-sided way, no longer being symmetric around the rotation axis. In addition, one side of the star is irradiated by the companion and may be heated. Although the system is synchronized, the tides continue to extract or deposit angular momentum from or onto the stars. How such effects, induced by the presence of the companion star, interact with the different rotational instabilities is not well understood and poses an additional uncertainty on our predictions. If such effects are important and lead to additional mixing, our predictions for the N surface abundance can still be used as a test for rotational mixing if they are considered as lower limits to the expected N abundance.

Avoiding mass transfer in short-period binaries

We have shown that rotational mixing, if it is as efficient as assumed in our models, can lead to chemically homogeneous evolution for tight binaries with a 50 $M_\odot$ primary. In these models the primary star stays so compact that the secondary star is the first to fill its Roche lobe.

This peculiar behavior of the radius of stars, which are efficiently mixed, has been noted in models of rapidly rotating massive single stars (Maeder 1987) and has been suggested as an evolutionary channel for the progenitors of long gamma-ray bursts (Yoon et al. 2006; Woosley & Heger 2006) in the collapsar scenario Woosley (1993). In single stars this type of evolution only occurs at low metallicity, because at solar metallicity mass

and angular momentum loss in the form of a stellar wind spins down the stars and prevents initially rapidly rotating stars from evolving chemically homogeneously (Yoon et al. 2006; Brott et al. 2009). In a close binary tides can replenish the angular momentum, opening the possibility for chemically homogeneous evolution in the solar neighborhood.

The binary models presented here all evolve into contact, but (as we discussed briefly in Sect. 5.2) Roche-lobe overflow may be avoided altogether in systems in which the secondary stays compact, either because it also evolves chemically homogeneously, which may occur if $M_1 \approx M_2$, or because it evolves on a much longer timescale than the primary, when $M_2 \ll M_1$. Whereas standard binary evolution theory predicts that the shorter the orbital period, the earlier mass transfer sets in, we find that binaries with the lowest orbital periods may avoid the onset of mass transfer altogether. This evolution scenario does not fit in the traditional classification of interacting binaries into Case *A*, *B* and *C*, based on the evolutionary stage of the primary component at the onset of mass transfer (Kippenhahn & Weigert 1967; Lauterborn 1970). In the remainder of this paper we will refer to this new case of binary evolution, in which mass transfer is delayed or avoided altogether as a result of very efficient internal mixing, as Case *M*.

The massive and tight systems in which Case *M* can occur are rare. Additional mixing processes induced by the presence of the companion star, which may be important in such systems, will widen the parameter space in which Case *M* can occur: it would lower the minimum mass for the primary star and increase the orbital period below which this type of evolution occurs. The massive LMC binary [L72] LH 54-425, with an orbital period of 2.25 d (Williams et al. 2008, see also Sect. 5.2) may be a candidate for this type of evolution. Another interesting case is the galactic binary WR20a, which consists of two core hydrogen burning stars of 82.7 ± 5.5 and $81.9 \pm 5.5\ M_\odot$ in an orbit of 3.69 d. Both stars are so compact that they are detached. The surface abundance show evidence of rotational mixing: a nitrogen abundance of six times solar is observed and carbon is depleted (Bonanos et al. 2004; Rauw et al. 2005).

Short-period Wolf-Rayet and black-hole binaries

If Roche-lobe overflow is avoided throughout the core hydrogen-burning phase of the primary star, both stars will stay compact while the primary gradually becomes a helium star and can be observed as a Wolf-Rayet star. Initially the Wolf-Rayet star will be more massive than its main sequence companion, but mass loss due to the strong stellar wind may reverse the mass ratio, especially in systems which started with nearly equal masses. Examples of observed short-period Wolf-Rayet binaries with a main-sequence companion are CQ Cep[8], CX Cep[9], HD 193576[10] and the very massive system HD 311884[11] (van der Hucht 2001). Such systems are thought to be the result of very non-conservative mass transfer or a common envelope phase (e.g. Petrovic et al. 2005a). Case M constitutes an alternative formation scenario which does not involve mass transfer.

Case *M* is also interesting in the light of massive black-hole binaries. Orosz et al. (2007) recently published the stellar parameters of M33 X-7, located in the nearby galaxy Messier 33 which harbors one of the most massive stellar black holes known to date, $M_{\rm bh} = 15.7 \pm 1.5\ M_\odot$, orbiting a massive O star, $M_{\rm O} = 70 \pm 7\ M_\odot$, which resides inside its Roche lobe in spite of the fact that the orbit is very tight, $P_{\rm orb} = 3.45$ d. The explanation for the formation of this system with standard binary evolutionary models involves a common-envelope phase that sets in after the end of core helium burning (Case *C*), as the progenitor of the black hole must have had a radius much greater than the current orbital separation. This scenario is problematic as it requires that the black-hole progenitor lost roughly ten times less mass before the onset of Roche-lobe overflow than what is currently predicted by stellar evolution models (Orosz et al. 2007). An additional problem is that the most likely outcome of the common envelope phase would be a merger, as the envelopes of massive stars are tightly bound (Podsiadlowski et al. 2003). In the Case *M* scenario the black-hole progenitor can stay compact and avoid Roche-lobe overflow at least until the end of core helium burning, such that it retains its envelope.

There are examples of stellar mass black-hole binaries with short periods and a massive main-sequence companion, in which nearly chemically homogeneous evolution may be important. IC 10 X-1 is a system harboring the most massive stellar mass black hole known to date with a mass of at least 21 $M_\odot$, orbiting a Wolf-Rayet star of approximately 25 $M_\odot$ in an orbit of 1.45 days (Silverman & Filippenko 2008). Homogeneous evolution helps to explain the high mass of the black hole, but the short orbital period poses a difficulty, also for Case *M*: strong mass loss during the Wolf-Rayet life time will widen the orbit. Other examples of high mass black hole binaries with short orbital periods are the famous systems Cyg X-1[12] (Herrero et al. 1995), LMC X-1[13] (Orosz et al. 2008) and LMC X-3[14] (Yao et al. 2005, and references therein).

The subsequent evolution of tight rapidly rotating Wolf-Rayet binaries remains to be investigated. If one or both members of the system can retain enough angular momentum to fulfill the collapsar scenario (Woosley 1993), which may be hard as the tides can slow down the stars (e.g. Detmers et al. 2008), it may lead to the production of one or even two long gamma-ray bursts.

Although promising, the importance of this channel may be small due to the limited binary parameter space in which Case *M* can occur. To make any strong statements about this new evolutionary scenario, further modeling is needed, which we will undertake in the near future.

7. Conclusion

We investigated the effect of rotational mixing on the evolution of detached short-period massive binaries using a state of the art stellar evolution code. The efficiency of rotational mixing was calibrated under the assumption that rotational mixing is the main process responsible for the observed N enhancements in rotating stars.

We find nitrogen surface enhancements of up to 0.6 dex for massive binaries in the SMC. The largest enhancements can be reached in systems with orbital periods less than about 2 days, in which the primary is massive (about 20 $M_\odot$ or more) and evolved (filling its Roche lobe by about 80% or more) and the secondary is significantly less massive, which leads to a more spacious Roche lobe for the primary (preferably $M_2/M_1 \lesssim 0.75$).

[8] CQ Cep: $M_{\rm WR} = 24\ M_\odot$, $M_{\rm O} = 30\ M_\odot$, $P_{\rm orb} = 1.6$ d.
[9] CX Cep: $M_{\rm WR} = 20\ M_\odot$, $M_{\rm O} = 28\ M_\odot$, $P_{\rm orb} = 2.1$ d.
[10] HD 193576: $M_{\rm WR} = 9\ M_\odot$, $M_{\rm O} = 29\ M_\odot$, $P_{\rm orb} = 4.2$ d.
[11] HD 311884: $M_{\rm WR} = 51\ M_\odot$, $M_{\rm O} = 60\ M_\odot$, $P_{\rm orb} = 6.2$ d.
[12] Cyg X-1: $M_{\rm bh} \approx 10\ M_\odot$, $M_{\rm O} \approx 18\ M_\odot$, $P_{\rm orb} = 5.6$ d.
[13] LMC X-1: $M_{\rm bh} \approx 10\ M_\odot$, $M_{\rm O} \approx 30\ M_\odot$, $P_{\rm orb} = 3.9$ d.
[14] LMC X-3: $M_{\rm bh} \approx 4$–$10\ M_\odot$, $M_{\rm O} \approx 40\ M_\odot$, $P_{\rm orb} = 4.2$ d.

We propose to use such systems as test cases for rotational mixing. These systems often show eclipses and big radial velocity variations, such that their stellar parameters, the rotation rate and possibly their surface abundances can be determined with high accuracy. This enables a direct comparison between an observed system and models computed with the appropriate stellar and binary parameters. An additional major advantage of using detached main-sequence binaries is the constraint on the evolutionary history. For a fast spinning apparently single star we do not know whether it was born as a fast rotator or whether its rotation rate is the result of mass transfer or merger event. In a detached main-sequence binary we can exclude the occurrence of any mass transfer phase since the onset of core-hydrogen burning (see Sect. 1).

In the most massive binaries we find that rotational instabilities can efficiently mix centrally produced helium throughout the stellar envelope of the primary. They follow the evolution for chemically homogeneous stars: they stay within their Roche lobe, being over-luminous and blue compared to normal stars. Due to large amount of nitrogen and helium at the surface these stars can be observed as Wolf-Rayet stars with hydrogen in their spectra. In contrast to standard binary evolution, we find that it is the less massive star in these systems that fills its Roche lobe first.

There may be regions in the binary parameter space in which Roche-lobe overflow can be avoided completely during the core hydrogen-burning phase of the primary. The parameter space for this new evolutionary scheme, which we denote Case *M* to emphasize the important role of mixing, increases if additional mixing processes play a role in such massive systems. It may provide an alternative channel for the formation or tight Wolf-Rayet binaries with a main-sequence companion, without the need for a mass transfer and common envelope phase to bring the stars close together. This scenario is also potentially interesting for tight massive black hole binaries, such as M33 X-7 (Orosz et al. 2007), for which no satisfactory evolutionary scenario exists to date.

Acknowledgements. The authors would like to thank G. Meynet (referee), E. Glebbeek, M, Verkoulen, K. Belzcinski, Z. Han, J.-P. Zahn and the members of the VLT-FLAMES consortium. The authors acknowledge NOVA and LKBF for financial support. S.-Ch. Y. is supported by the DOE SciDAC Program (DOE DE-FC02-06ER41438).

References

Alongi, M., Bertelli, G., Bressan, A., et al. 1993, A&AS, 97, 851
Asplund, M., Grevesse, N., & Sauval, A. J. 2005, in Cosmic Abundances as Records of Stellar Evolution and Nucleosynthesis, ed. T. G. Barnes, III & F. N. Bash, ASP Ser., 336, 25
Belczynski, K., Kalogera, V., & Bulik, T. 2002, ApJ, 572, 407
Bonanos, A. Z., Stanek, K. Z., Udalski, A., et al. 2004, ApJ, 611, L33
Bouret, J.-C., Lanz, T., Hillier, D. J., et al. 2003, ApJ, 595, 1182
Brookshaw, L., & Tavani, M. 1993, ApJ, 410, 719
Brott, I., Langer, N., Lennon, D., et al. 2009, in prep.
Cantiello, M., Yoon, S.-C., Langer, N., & Livio, M. 2007, A&A, 465, L29
Cantiello, M., Langer, N., Brott, I., et al. 2009, A&A, submitted
Daflon, S., Cunha, K., Butler, K., & Smith, V. V. 2001, ApJ, 563, 325
De Mink, S. E., Pols, O. R., & Hilditch, R. W. 2007, A&A, 467, 1181
Detmers, R. G., Langer, N., Podsiadlowski, P., & Izzard, R. G. 2008, A&A, 484, 831
Domiciano de Souza, A., Kervella, P., Jankov, S., et al. 2003, A&A, 407, L47
Eddington, A. S. 1925, The Observatory, 48, 73
Eddington, A. S. 1926, The Internal Constitution of the Stars (Cambridge University Press)
Eggleton, P. P. 1983, ApJ, 268, 368
Evans, C. J., Smartt, S. J., Lee, J.-K., et al. 2005, A&A, 437, 467
Fliegner, J., Langer, N., & Venn, K. A. 1996, A&A, 308, L13
Friend, D. B., & Abbott, D. C. 1986, ApJ, 311, 701
Gies, D. R., & Lambert, D. L. 1992, ApJ, 387, 673
Harries, T. J., Hilditch, R. W., & Howarth, I. D. 2003, MNRAS, 339, 157
Heger, A., & Langer, N. 2000, ApJ, 544, 1016
Heger, A., Langer, N., & Woosley, S. E. 2000, ApJ, 528, 368
Heger, A., Woosley, S. E., & Spruit, H. C. 2005, ApJ, 626, 350
Herrero, A., Kudritzki, R. P., Gabler, R., Vilchez, J. M., & Gabler, A. 1995, A&A, 297, 556
Hilditch, R. W., Howarth, I. D., & Harries, T. J. 2005, MNRAS, 357, 304
Huang, W., & Gies, D. R. 2006, ApJ, 648, 591
Hunter, I., Dufton, P. L., Smartt, S. J., et al. 2007, A&A, 466, 277
Hunter, I., Brott, I., Lennon, D. J., et al. 2008, ApJ, 676, L29
Hurley, J. R., Tout, C. A., & Pols, O. R. 2002, MNRAS, 329, 897
Iglesias, C. A., & Rogers, F. J. 1996, ApJ, 464, 943
Kippenhahn, R., & Weigert, A. 1967, Zeitschrift fur Astrophysik, 65, 251
Korn, A. J., Keller, S. C., Kaufer, A., et al. 2002, A&A, 385, 143
Langer, N. 1991, A&A, 252, 669
Langer, N. 1998, A&A, 329, 551
Langer, N., Cantiello, M., Yoon, S.-C., et al. 2008, in IAU Symp., 250, 167
Lauterborn, D. 1970, A&A, 7, 150
Leushin, V. V. 1988, Sov. Astron., 32, 430
Maeder, A. 1987, A&A, 178, 159
Maeder, A., & Meynet, G. 2000a, A&A, 361, 159
Maeder, A., & Meynet, G. 2000b, ARA&A, 38, 143
Martins, F., Hillier, D. J., Bouret, J. C., et al. 2008, ArXiv e-prints
Massey, P., Penny, L. R., & Vukovich, J. 2002, ApJ, 565, 982
Mendel, J. T., Venn, K. A., Proffitt, C. R., Brooks, A. M., & Lambert, D. L. 2006, ApJ, 640, 1039
Meynet, G., & Maeder, A. 1997, A&A, 321, 465
Mokiem, M. R., de Koter, A., Evans, C. J., et al. 2007, A&A, 465, 1003
Nelson, C. A., & Eggleton, P. P. 2001, ApJ, 552, 664
Orosz, J. A., McClintock, J. E., Narayan, R., et al. 2007, Nature, 449, 872
Orosz, J. A., Steeghs, D., McClintock, J. E., et al. 2008, ArXiv e-prints
Pavlovski, K., & Hensberge, H. 2005, A&A, 439, 309
Petrovic, J., Langer, N., & van der Hucht, K. A. 2005a, A&A, 435, 1013
Petrovic, J., Langer, N., Yoon, S.-C., & Heger, A. 2005b, A&A, 435, 247
Podsiadlowski, P., Joss, P. C., & Hsu, J. J. L. 1992, ApJ, 391, 246
Podsiadlowski, P., Rappaport, S., & Han, Z. 2003, MNRAS, 341, 385
Pols, O. R. 1994, A&A, 290, 119
Rauw, G., Crowther, P. A., De Becker, M., et al. 2005, A&A, 432, 985
Schnurr, O., Moffat, A. F. J., St-Louis, N., Morrell, N. I., & Guerrero, M. A. 2008, MNRAS, 389, 806
Schroder, K.-P., Pols, O. R., & Eggleton, P. P. 1997, MNRAS, 285, 696
Silverman, J. M., & Filippenko, A. V. 2008, ApJ, 678, L17
Spruit, H. C. 2002, A&A, 381, 923
Stothers, R. B., & Chin, C.-W. 1992, ApJ, 390, 136
Suijs, M. P. L., Langer, N., Poelarends, A.-J., et al. 2008, A&A, 481, 87
Toledano, O., Moreno, E., Koenigsberger, G., Detmers, R., & Langer, N. 2007, A&A, 461, 1057
van der Hucht, K. A. 2001, New Astron. Rev., 45, 135
Vanbeveren, D., Van Bever, J., & Belkus, H. 2007, ApJ, 662, L107
Venn, K. A., Brooks, A. M., Lambert, D. L., et al. 2002, ApJ, 565, 571
Vogt, H. 1925, Astron. Nachr., 223, 229
von Zeipel, H. 1924, MNRAS, 84, 665
Walborn, N. R. 1976, ApJ, 205, 419
Walborn, N. R., Morrell, N. I., Howarth, I. D., et al. 2004, ApJ, 608, 1028
Wellstein, S., & Langer, N. 1999, A&A, 350, 148
Wellstein, S., Langer, N., & Braun, H. 2001, A&A, 369, 939
Williams, S. J., Gies, D. R., Henry, T. J., et al. 2008, ApJ, 682, 492
Witte, M. G., & Savonije, G. J. 1999, A&A, 350, 129
Woosley, S. E. 1993, ApJ, 405, 273
Woosley, S. E., & Heger, A. 2006, ApJ, 637, 914
Yao, Y., Wang, Q. D., & Nan Zhang, S. 2005, MNRAS, 362, 229
Yoon, S.-C., & Langer, N. 2005, A&A, 443, 643
Yoon, S.-C., Langer, N., & Norman, C. 2006, A&A, 460, 199
Zahn, J.-P. 1974, in Stellar Instability and Evolution, ed. P. Ledoux, A. Noels, & A. W. Rodgers, IAU Symp., 59, 185
Zahn, J.-P. 1975, A&A, 41, 329
Zahn, J.-P. 1977, A&A, 57, 383
Zahn, J.-P. 1989, A&A, 220, 112